

# Easy, Interpretable, Effective: openSMILE for voice deepfake detection

Octavian Pascu

POLITEHNICA Bucharest

octavian.pascu@upb.ro

Dan Oneatǎ

POLITEHNICA Bucharest

dan.oneata@gmail.com

Horia Cucu

POLITEHNICA Bucharest

horia.cucu@upb.ro

Nicolas Müller

FRAUNHOFER AISEC, Germany

nicolas.mueller@aisec.fraunhofer.de

**Abstract**—In this paper, we demonstrate that attacks in the latest ASVspoof5 dataset—a de facto standard in the field of voice authenticity and deepfake detection—can be identified with surprising accuracy using a small subset of very simplistic features. These are derived from the openSMILE library, and are scalar-valued, easy to compute, and human interpretable. For example, attack A10’s unvoiced segments have a mean length of  $0.09 \pm 0.02$ , while bona fide instances have a mean length of  $0.18 \pm 0.07$ . Using this feature alone, a threshold classifier achieves an Equal Error Rate (EER) of 10.3% for attack A10. Similarly, across all attacks, we achieve up to 0.8% EER, with an overall EER of  $15.7 \pm 6.0\%$ .

We explore the generalization capabilities of these features and find that some of them transfer effectively between attacks, primarily when the attacks originate from similar Text-to-Speech (TTS) architectures. This finding may indicate that voice anti-spoofing is, in part, a problem of identifying and remembering signatures or fingerprints of individual TTS systems. This allows to better understand anti-spoofing models and their challenges in real-world application.

## I. INTRODUCTION

Text-to-speech (TTS) technology has advanced significantly in recent years, offering various beneficial applications, such as the restoration of voice capabilities for speech-impaired individuals [1]. Despite these positive developments, TTS also presents potential risks such as the compromise of voice biometric systems and the creation of deepfakes, which enable fraud, slander and misinformation. A key initiative in combating these threats is the ASVspoof Challenge [2]. Since its inception in 2015, this biennial event has released datasets crucial for the design of anti-spoofing systems. Notably, since the forth iteration of ASVspoof in 2021 [3], [4], the challenge has included a separate track specifically for detecting audio deepfakes. The latest iteration of the ASVspoof challenge dataset is called ‘ASVspoof 5’, and is set to succeed the ASVspoof 2021 dataset, the de-facto standard in evaluating of voice authenticity systems.

While related work reports high performance on the ASVspoof datasets [5]–[7], achieving true generalization that applies effectively in real-world scenarios remains a challenge. Existing studies suggest that anti-spoofing efforts often rely on shortcut artifacts, such as the length of silences [8] or bitrate information [9], and struggle with cross-dataset generalization [10]. Large self-supervised representations improve the generalization to some degree [11], but this approach comes at the cost of explainability, which remains an important desideratum given the decision-critical nature of deepfake detection.

In this work, we propose to use openSMILE [12], a software tool for the automatic extraction of audio features. This tool allows the computation of interpretable features, based on fundamental properties such as the length of voiced and unvoiced segments, spectral flux (a measure of how quickly the power spectrum of a signal is changing), or energy within specific frequency ranges. Our findings demonstrate that for the ASVspoof5 dataset, even single, scalar-valued openSMILE features allow for surprisingly accurate classification of attacks (i.e. voice deepfakes from a specific TTS system). For example, the ‘MeanUnvoiceSegmentLength’ feature allows for reliable identification

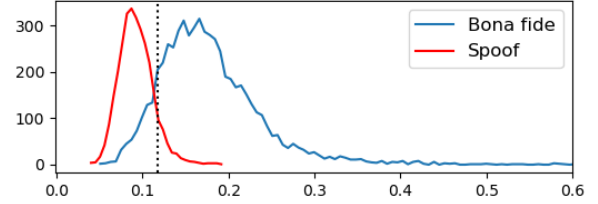


Fig. 1. Distribution of the openSMILE ‘eGeMAPSv2’ feature F85, ‘MeanUnvoicedSegmentLength’, computed for attack A10 and bona fide data from ASVspoof5. A simple threshold classifier obtains an EER of 10.3% by predicting ‘spoof’ if  $F85 < 0.12$ , else ‘bona fide’ (dotted line).

of attack A10, c.f. Figure 1. We find that for each attack in ASVspoof5, such features can be found. Interestingly, the features extracted exhibit varying degrees of specificity: some are highly specific and fail to generalize across different types of attacks, while others show broader applicability. This variation suggests that the underlying text-to-speech (TTS) models each possess unique characteristics that, if recognized during training, facilitate identification. In summary:

- We employ openSMILE to identify single, scalar-valued and human-interpretable features that effectively pinpoint attacks within the ASVspoof5 dataset.
- We show that cross-domain generalization works best when attacks come from similar TTS architectures.
- This observation suggests that TTS models exhibit unique characteristics, akin to fingerprints, which are readily identifiable if seen during training, but can pose significant challenges in cross-model generalization.

## II. METHODOLOGY

### A. Data Partitioning

We utilize the two currently available, labeled partitions of the ASVspoof5 [13] dataset: ‘train’ and ‘dev’. Each partition a set of bona fide instances, denoted as  $BT$  and  $BD$  (bona fide ‘train’ and bona fide ‘dev’, respectively). Additionally, each partition includes spoofed audio files, categorized by the TTS system used to generate them, referred to as ‘attacks’. The ‘train’ partition comprises attacks A01 through A08, while the ‘dev’ partition includes attacks A09 through A16; the types of attacks are listed in Table II. For our experiments, we divided  $BT$  and  $BD$ , along with each attack, into an 80% training pool and a 20% evaluation pool, c.f. Figure 2.

### B. Identifying Predictive openSMILE Features

Our objective is to ascertain whether attacks in ASVspoof5 can be detected using a single, scalar-valued feature from openSMILE. We aim to evaluate the performance of this method in both in-domain (ID) and out-of-domain (OOD) scenarios. ID scenarios

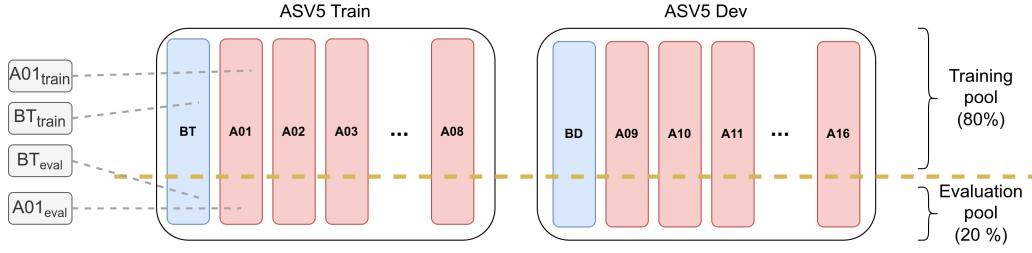


Fig. 2. Visualization of the ASVspoof5 dataset’s ‘train’ and ‘dev’ partition. BT and BD correspond to the respective bona fide data, while A01 through A16 correspond to the individual attacks. Grey boxes on the left indicate the naming convention we use in subsequent experiments.

involve training and evaluation data from the same attack, whereas OOD scenarios involve training and evaluation data from different attacks. For instance, consider a classifier trained on bona fide instances from the training pool ( $BD_{\text{train}}$  and  $BT_{\text{train}}$ ), as well as spoofed instances from attack  $A01_{\text{train}}$ . Evaluating performance on  $BD_{\text{eval}}$ ,  $BT_{\text{eval}}$ , and  $A01_{\text{eval}}$  constitutes an ID challenge, while evaluating performance on  $BD_{\text{eval}}$ ,  $BT_{\text{eval}}$ , and  $A02_{\text{eval}}$  constitutes an OOD challenge. Prior research [10], [14], [15] highlights that OOD generalization is challenging but essential for real-world deepfake detection applications.

We aim to identify the most predictive features for each attack  $A_j$ . To this end, we utilize openSMILE’s ‘eGmapsV2’ feature set [16], consisting of 88 scalar-valued features derived from an audio’s loudness, spectral flux, voiced and unvoiced segment lengths, etc. This set is an extended version of the Geneva Minimalistic Acoustic Parameter (eGeMAPS) feature set, originally employed for emotion recognition and affective computing. While we have considered other feature sets, such as ‘emobase’, we found them to be less interpretable.

To illustrate our approach, consider Figure 1. The plot shows the distribution of the feature ‘MeanUnvoicedSegmentLength’ (shorthand  $F85$ , being the 86th feature from ‘eGeMAPSv2’) for bona fide instances and attack A10. The red line represents spoofed data from A10, while the blue line represents bona fide data from the ‘train’ and ‘dev’ splits. It is evident that this feature exhibits distinct behavior between spoofed and real data. For spoofed data, this feature assumes values of  $0.09 \pm 0.02$  (mean and standard deviation, respectively), while for bona fide data, it assumes values of  $0.18 \pm 0.07$ . Using this feature as a predictor, a threshold classifier achieves an EER of 10.3%, much better than random guessing (50% EER). Therefore, ‘MeanUnvoicedSegmentLength’ is a good predictor for attack A10. In subsequent experiments, we find the most predictive features using this approach: For each attack  $A_j$  and each ‘eGeMAPSv2’ feature, compute the EER on  $BT_{\text{train}}$ ,  $BD_{\text{train}}$ , and  $A_{j\text{train}}$ . Then, we present the two features that individually yield the best EER.

### III. EXPERIMENTS

#### A. Experiment A: openSMILE, In-domain

In this initial experiment, we evaluate the effectiveness of ‘eGeMAPSv2’ in an in-domain (ID) setting, where the training and testing data originate from the same distribution.

First, we select the front-end: as outlined in Section II-B, we identify the two most predictive features per attack. Second, we train the back-end on each feature individually: A linear classification model  $f(x) = wx + b \in \mathbb{R}$  where  $x, w, b \in \mathbb{R}$ . This model is trained on the ‘train’ portion of the attack data along with the bona fide training data (i.e.  $BD_{\text{train}}$ ,  $BT_{\text{train}}$  and  $A_{j\text{train}}$ , c.f. Figure 2). We then compute the EER on the corresponding evaluation data, i.e.  $BD_{\text{eval}}$ ,  $BT_{\text{eval}}$  and  $A_{j\text{eval}}$ .

TABLE I  
IN-DOMAIN TEST PERFORMANCE PER ATTACK, FOR THE TOP-2 FEATURES PER ATTACK A01 THROUGH A16.

Attack	Feature	Test EER	Attack	Feature	Test EER
A01	F66	12.8	A09	F86	8.0
	F19	13.8		F85	11.5
A02	F66	12.7	A10	F86	7.3
	F19	13.0		F85	10.7
A03	F19	15.3	A11	F58	15.3
	F66	15.7		F60	15.3
A04	F19	16.8	A12	F82	18.2
	F21	17.3		F19	21.3
A05	F21	17.5	A13	F67	22.1
	F19	19.4		F39	22.8
A06	F21	16.8	A14	F45	0.8
	F19	17.1		F51	0.8
A07	F66	13.7	A15	F78	20.7
	F1	14.2		F77	25.7
A08	F20	17.7	A16	F66	23.8
	F66	18.2		F18	26.8

Table I presents the results for in-domain evaluation. For most attacks, a single openSMILE feature is sufficient to achieve good performance, with results as low as 0.8% EER for attack A14. The worst performance is observed for attack A16, where the best performing feature  $F66$  yields an EER of 23.8%. On average, this simplistic approach achieves  $15.7 \pm 6.0\%$  EER—much better than random guessing.

These results indicate that each attack has a distinctive fingerprint, and is characterized by unique, but simplistic patterns. While some attacks are more easily identified than others, this principle holds throughout ASVspoof5. Interestingly, certain features, such as  $F19$ , are effective across multiple attacks (7 out of 16 attacks), whereas others, like  $F51$ , are highly effective for specific attacks (e.g., A14 with 0.8% EER) but not for others. Some of the most occurring features in Table I are:

- **F19 (7 occurrences):** loudness\_sma3\_stddevFallingSlope – standard deviation of the falling slope of the simple moving average (with a window size of 3) of the loudness.
- **F66 (6 occurrences):** spectralFluxV\_sma3nz\_amean – arithmetic mean of the simple moving average (with a window size of 3) of the spectral flux for non-zero values.
- **F85 (2 occurrences):** MeanUnvoicedSegmentLength – average length of all unvoiced segments within the audio file.
- **F86 (2 occurrences):** StddevUnvoicedSegmentLength – standard deviation of the length of all unvoiced segments.

TABLE II  
TTS SYSTEM PER SPOOFING ATTACK, AS PRESENTED IN [13].

Attack	System	Attack	System
A01	GlowTTS [17]	A09	ToucanTTS [18]
A02	Variant of A01	A10	A09+HiFiGANv2 [19]
A03	Variant of A01	A11	Tacotron2 [20]
A04	GradTTS [21]	A12	In-house unit-select
A05	Variant of A04	A13	StarGANv2-VC [22]
A06	Variant of A04	A14	YourTTS [23]
A07	FastPitch [24]	A15	VAE-GAN [25]
A08	VITS [26]	A16	In-house ASR-based

### B. Experiment B: openSMILE, Out-of-domain

In our second experiment, we extend our approach to an out-of-domain (OOD) setting, where the training and testing data come from different distributions. This aims to evaluate the effectiveness of openSMILE features for cross-domain detection in the ASVspoof5 dataset. We follow the same training protocol as in Section III-A, but evaluate on OOD data. For instance, given a model trained on A01, we evaluate on A02 through A16 and present the EERs individually. Note that both the feature itself, as well as the parameters  $w, b \in \mathbb{R}$  are derived from the initial in-domain training. This approach results in a matrix of OOD performances, where the entries on the diagonal correspond to the in-domain (ID) values, as shown in Table I.

The results are shown in Table III, where the rows indicate the training attack, and the columns indicate the evaluation attack. Note that Table III can be partitioned into four sub-matrices based on the ‘train’ and ‘dev’ partitions of the ASVspoof 5 dataset. Systems trained on attacks A01 through A08 generalize relatively well to other ‘train’ attacks, as indicated by the green highlights and correspondingly lower EERs ( $20.0 \pm 7.0\%$ ) in the top-left quadrant.

We observe that certain groups of attacks exhibit strong generalization between themselves, such as A09 and A10 ( $9.3 \pm 1.7\%$  EER). We hypothesize that this generalization is due to similarities in the underlying TTS algorithms (see Table II for details). For example, both A09 and A10 are derived from ToucanTTS [18], which explains their effective generalization. Similarly, A01, A02, and A03 are based on the GlowTTS architecture [17], which likely contributes to the strong generalization observed among them. Generalization across different TTS architectures often proves challenging; for example, systems trained on A16 do not generalize to any of the attacks from A01 through A08.

In summary, generalization from ‘dev’ to ‘train’ and vice-versa is challenging, as indicated by the predominantly red highlights and high EERs ( $52.9 \pm 17.9\%$ ) in the bottom-left and top-right quadrants.

### C. Experiment C: Comparison with Neural Front-end

We compare the ‘eGeMAPSv2’ openSMILE front-end to the Wav2Vec2<sup>1</sup> self-supervised neural front-end [27], used widely in related work [11], [28]–[32]. For each of the 768 scalar outputs of Wav2Vec2, we assess how discriminative it is for each of the sixteen attacks in ASV5. This is done by using the scalar value as a score itself and directly computing the EER on them, similar to Figure 1. Thus, for each attack, we obtain 768 predictors with corresponding EERs. We perform the same process for openSMILE and compare via a (normalized) distribution plot, c.f. Figure 3. We observe that for both openSMILE and Wav2Vec2, many of the features are not predictive: the performance has its mode around 40–50% EER. However, for both feature sets there is a small subset of more predictive features

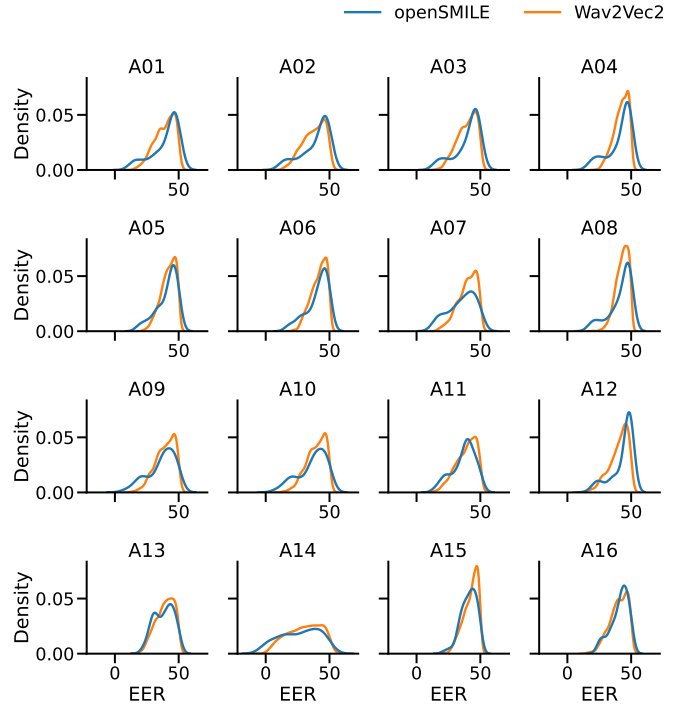


Fig. 3. Distribution plot comparing the performance of scalar-valued features extracted using openSMILE (blue) and Wav2Vec2 (orange) across attacks A01 to A16. The  $x$ -axis represents the EER obtained by each feature, and the  $y$ -axis denotes frequency. The plot reveals that openSMILE features sometimes exhibit higher predictive accuracy, as evidenced by a greater concentration of distributional mass near an  $EER = 0$ .

(around 20–30% EER). Note that this subset is much more distinct for openSMILE, which tends to exhibit a bimodal distribution for some attacks (e.g., A04, A08, A09, A13). Note also the attack A14, unlike other attacks, seems to be easily detectable by many of its features, as indicated by the high distributional mass at  $EER = 0$ .

We train a logistic regression classifier on all features for both openSMILE and Wav2Vec2. Similar to the experiments in Section III-B, we consider all combinations of train–test attacks, that is, we train on one attack and evaluate on all others. However, for brevity, we report only aggregated results for the two main cases: in domain (when train and test attacks match), and out of domain (when train and test attacks do not match). The results are shown in Table IV. Here, we observe the reverse trend to the previous experiment: Wav2Vec2 gives better performance than openSMILE for both in-domain and out-of-domain configuration. Thus, while individual features of Wav2Vec2 are not as predictive, they do perform much better as a whole. We also see that using all features for openSMILE significantly improves performance over the single features in both Table I and Table III.

## IV. RELATED WORK

Kumar *et al.* [33] use openSMILE’s ‘eGeMAPSv2’ as a front-end, combined with traditional machine learning models such as decision trees or linear regression, and evaluate on three datasets: CMU Arctic [34], LibriTTS [35], and the LJ Speech [36] dataset. The corresponding spoofed audio files are created by themselves. Their results support our finding that in an ID setting, openSMILE front-ends work very reliably, while OOD performance degenerates to random guessing. Similar results are obtained by Sadashiv *et al.* [37], who evaluate on ASVspoof 2019 [38] in addition to CMU Arctic, LJ

<sup>1</sup>huggingface.co/facebook/wav2vec2-base

TABLE III

OUT-OF-DOMAIN EVALUATION RESULTS PRESENTED IN TERMS OF EER. ROWS INDICATE TRAINING ATTACK AND OPENSMILE FEATURE USED, WHILE COLUMNS INDICATE EVALUATION ATTACK. NOTE THAT THE VALUES ON THE DIAGONAL ORIGINATE FROM IDENTICAL TRAIN AND TEST ATTACKS, AND THUS REPRESENT IN-DOMAIN EVALUATION.

Attack ↓	Feature ↓	ASVspoof 5 'train'								ASVspoof 5 'dev'							
		A01	A02	A03	A04	A05	A06	A07	A08	A09	A10	A11	A12	A13	A14	A15	A16
A01	F66	12.8	12.7	15.7	21.7	31.5	25.7	13.7	18.2	68.7	69.5	68.1	70.3	60.0	55.2	68.7	76.2
	F19	13.8	13.0	15.3	16.8	19.4	17.1	17.8	23.0	61.9	62.8	55.7	78.7	54.7	54.5	65.3	66.7
A02	F66	12.8	12.7	15.7	21.7	31.5	25.7	13.7	18.2	68.7	69.5	68.1	70.3	60.0	55.2	68.7	76.2
	F19	13.8	13.0	15.3	16.8	19.4	17.1	17.8	23.0	61.9	62.8	55.7	78.7	54.7	54.5	65.3	66.7
A03	F19	13.8	13.0	15.3	16.8	19.4	17.1	17.8	23.0	61.9	62.8	55.7	78.7	54.7	54.5	65.3	66.7
	F66	12.8	12.7	15.7	21.7	31.5	25.7	13.7	18.2	68.7	69.5	68.1	70.3	60.0	55.2	68.7	76.2
A04	F19	13.8	13.0	15.3	16.8	19.4	17.1	17.8	23.0	61.9	62.8	55.7	78.7	54.7	54.5	65.3	66.7
	F21	21.9	21.6	24.8	17.3	17.5	16.8	18.7	45.7	18.1	17.5	40.0	43.7	33.8	28.6	36.5	41.5
A05	F21	21.9	21.6	24.8	17.3	17.5	16.8	18.7	45.7	18.1	17.5	40.0	43.7	33.8	28.6	36.5	41.5
	F19	13.8	13.0	15.3	16.8	19.4	17.1	17.8	23.0	61.9	62.8	55.7	78.7	54.7	54.5	65.3	66.7
A06	F21	21.9	21.6	24.8	17.3	17.5	16.8	18.7	45.7	18.1	17.5	40.0	43.7	33.8	28.6	36.5	41.5
	F19	13.8	13.0	15.3	16.8	19.4	17.1	17.8	23.0	61.9	62.8	55.7	78.7	54.7	54.5	65.3	66.7
A07	F66	12.8	12.7	15.7	21.7	31.5	25.7	13.7	18.2	68.7	69.5	68.1	70.3	60.0	55.2	68.7	76.2
	F1	32.9	31.0	29.5	37.0	29.0	32.7	14.2	34.4	34.8	34.3	50.7	49.6	28.8	20.3	33.8	35.6
A08	F20	17.2	17.2	18.8	28.2	36.1	30.9	19.9	17.7	77.7	79.0	69.2	70.9	60.8	89.0	67.5	72.7
	F66	12.8	12.7	15.7	21.7	31.5	25.7	13.7	18.2	68.7	69.5	68.1	70.3	60.0	55.2	68.7	76.2
A09	F86	26.3	22.3	23.9	28.2	23.3	24.2	20.6	49.8	8.0	7.3	61.5	38.0	49.0	65.0	45.5	43.3
	F85	38.3	40.0	36.2	38.3	36.2	37.5	29.5	53.9	11.5	10.7	63.2	34.7	68.0	97.0	46.8	45.0
A10	F86	26.3	22.3	23.9	28.2	23.3	24.2	20.6	49.8	8.0	7.3	61.5	38.0	49.0	65.0	45.5	45.0
	F85	38.3	40.0	36.2	38.3	36.2	37.5	29.5	53.9	11.5	10.7	63.2	34.7	68.0	97.0	46.8	43.3
A11	F58	48.6	50.3	49.3	49.3	44.3	42.7	41.4	48.0	36.5	38.2	15.3	51.3	50.8	54.8	38.9	49.7
	F60	46.2	48.0	46.0	48.8	43.5	40.7	40.3	46.3	35.6	37.8	15.3	52.6	49.0	58.7	37.3	40.7
A12	F82	34.1	33.6	36.2	29.3	29.6	28.7	47.6	60.2	36.6	34.3	64.5	18.2	66.1	94.0	43.2	51.3
	F19	86.2	87.0	84.7	83.3	80.6	82.9	82.2	77.0	38.1	37.3	44.3	21.3	45.3	45.5	34.8	33.3
A13	F67	32.0	30.6	34.1	25.0	24.6	25.3	24.8	39.0	40.7	39.7	33.2	49.5	22.1	15.0	38.1	35.8
	F39	36.1	33.3	37.3	42.5	33.7	33.4	25.8	37.9	38.4	40.5	28.7	49.3	22.8	20.1	36.8	33.0
A14	F45	52.8	53.3	56.9	46.7	50.4	48.1	71.2	55.6	80.9	80.8	39.9	41.8	32.1	0.8	45.6	55.0
	F51	51.0	51.0	54.3	44.8	45.2	42.3	65.0	53.2	73.8	73.8	34.3	43.0	29.3	0.8	42.0	56.0
A15	F78	56.2	59.7	57.7	55.7	52.2	53.2	57.8	49.0	43.2	44.7	41.2	51.8	62.7	58.5	20.7	45.3
	F77	49.6	49.8	50.3	48.8	48.0	47.6	55.3	45.2	48.2	48.9	22.6	46.0	58.3	31.3	25.7	43.8
A16	F66	87.2	87.3	84.3	78.3	68.5	74.3	86.3	81.8	31.3	30.5	31.9	29.7	40.0	44.8	31.3	23.8
	F18	81.0	82.2	79.2	73.7	69.2	73.8	77.1	76.5	31.2	29.5	42.3	24.3	46.3	37.8	34.4	26.8

TABLE IV

COMPARISON OF AGGREGATED ID AND OOD PERFORMANCE BETWEEN OPENSMILE AND WAV2VEC2 FEATURES.

Attack	In-domain test EER		Out-of-domain test EER	
	openSMILE	W2V2	openSMILE	W2V2
A01	1.6	0.0	41.9	5.5
A02	0.6	0.0	40.2	4.8
A03	1.7	0.0	38.9	4.7
A04	1.4	0.3	33.9	14.3
A05	1.0	0.3	26.7	15.6
A06	1.3	0.2	27.5	13.5
A07	0.3	0.0	37.2	13.1
A08	5.0	0.0	41.6	9.3
A09	2.6	0.0	34.7	13.1
A10	2.1	0.2	35.2	11.1
A11	0.7	0.0	30.7	14.8
A12	8.5	0.2	50.1	25.3
A13	2.5	0.5	33.7	16.0
A14	0.0	0.0	38.5	18.8
A15	6.5	0.5	41.6	8.1
A16	3.3	0.0	33.8	9.1

Speech, and LibriTTS. Other interpretable features such as energy, distortion, loudness have been used by Müller *et al.* [39] in the context of source tracing. Furthermore, frequency-based features such as fundamental frequency (F0) [40] and frequency sub-band [41]–[44] have been shown to be useful. Finally, a signal's noise (high-frequency

information) can also be used for voice anti-spoofing [44].

## V. DISCUSSION AND CONCLUSION

In this work, we analyze the efficacy of openSMILE as a front-end for voice anti-spoofing, specifically on the ASVspoof5 dataset. We find that for all attacks, there exist scalar-valued, human interpretable features which allow for good in-domain detection performance. However, the application of these characteristics in out-of-domain settings remains limited, particularly across different TTS architectures.

We argue that TTS models display unique characteristics, akin to a fingerprint, which can be readily identified once encountered but can have limited use for generalization across different models. Judging by the good transferability between attacks originating from similar TTS architectures, c.f. Table II and Table III, these characteristics appear to include information about the underlying TTS architecture. Conversely, generalization across architecture boundaries is challenging. Success in the field of source tracing [39], [45], which involves assigning instances to their generating models, further demonstrates that individual models exhibit individual characteristics. Thus, voice anti-spoofing may, in part, involve the challenge of identifying the unique signatures or fingerprints of individual TTS systems. While these distinctive characteristics can enable good identification of an attack, they require that the TTS model has been encountered during training. This may in part explain challenges in real-world application [10].



## REFERENCES

- [1] F. Biadsy, R. J. Weiss, P. J. Moreno, D. Kanvesky, and Y. Jia, "Parrottron: An end-to-end speech-to-speech conversion model and its applications to hearing-impaired speech and speech separation," in *Proc. Interspeech*, 2019, pp. 4115–4119.
- [2] Z. Wu, J. Yamagishi, T. Kinnunen, C. Hanilçi, M. Sahidullah, A. Sizov, N. Evans, M. Todisco, and H. Delgado, "ASVspoof: The automatic speaker verification spoofing and countermeasures challenge," *IEEE J. Sel. Top. Signal Process.*, vol. 11, no. 4, pp. 588–604, 2017.
- [3] J. Yamagishi, X. Wang, M. Todisco, M. Sahidullah, J. Patino, A. Nautsch, X. Liu, K. A. Lee, T. Kinnunen, N. W. D. Evans, and H. Delgado, "ASVspoof 2021: Accelerating progress in spoofed and deepfake speech detection," in *ASVspoof 2021 Workshop*, 2021.
- [4] X. Liu, X. Wang, M. Sahidullah, J. Patino, H. Delgado, T. Kinnunen, M. Todisco, J. Yamagishi, N. W. D. Evans, A. Nautsch, and K. A. Lee, "ASVspoof 2021: Towards spoofed and deepfake speech detection in the wild," *IEEE ACM Trans. Audio Speech Lang. Process.*, vol. 31, pp. 2507–2522, 2023.
- [5] H. Tak, J. Patino, M. Todisco, A. Nautsch, N. Evans, and A. Larcher, "End-to-end anti-spoofing with RawNet2," in *Proc. ICASSP*, 2021, pp. 6369–6373.
- [6] J.-w. Jung, H.-S. Heo, H. Tak, H.-j. Shim, J. S. Chung, B.-J. Lee, H.-J. Yu, and N. Evans, "AASIST: Audio anti-spoofing using integrated spectro-temporal graph attention networks," in *Proc. ICASSP*, 2022, pp. 6367–6371.
- [7] P. Kawa, M. Plata, M. Czuba, P. Szymanski, and P. Syga, "Improved deepfake detection using whisper features," in *Proc. Interspeech*, 2023, pp. 4009–4013.
- [8] N. M. Müller, F. Dieckmann, P. Czempin, R. Canals, K. Böttinger, and J. Williams, "Speech is silver, silence is golden: What do ASVspoof-trained models really learn?" in *Proc. ASVspoof 2021 Workshop*, 2021.
- [9] S. Borzi, O. Giudice, F. Stanco, and D. Allegra, "Is synthetic voice detection research going into the right direction?" in *Proc. CVPR Workshops*, 2022, pp. 71–80.
- [10] N. M. Müller, P. Czempin, F. Dieckmann, A. Froghyar, and K. Böttinger, "Does audio deepfake detection generalize?" in *Proc. Interspeech*, 2022, pp. 2783–2787.
- [11] O. Pascu, A. Stan, D. Oneata, E. Oneata, and H. Cucu, "Towards generalisable and calibrated synthetic speech detection with self-supervised representations," in *Proc. Interspeech*, 2024.
- [12] F. Eyben, M. Wöllmer, and B. Schuller, "OpenSMILE: The Munich versatile and fast open-source audio feature extractor," in *Proc. ACM MM*, 2010, pp. 1459–1462.
- [13] X. Wang, H. Delgado, H. Tak, J. weon Jung, H. jin Shim, M. Todisco, I. Kukanov, X. Liu, M. Sahidullah, T. Kinnunen, N. Evans, K. A. Lee, and J. Yamagishi, "ASVspoof 5: Crowdsourced data, deepfakes and adversarial attacks at scale," in *ASVspoof 2024 Workshop*, 2024.
- [14] L. Cuccovillo, C. Papastergiopoulos, A. Vafeiadis, A. Yaroshchuk, P. Aichroth, K. Votis, and D. Tzovaras, "Open challenges in synthetic speech detection," in *Proc. WIFS*, 2022, pp. 1–6.
- [15] J. Yi, C. Wang, J. Tao, X. Zhang, C. Y. Zhang, and Y. Zhao, "Audio deepfake detection: A survey," *CoRR*, vol. abs/2308.14970, 2023.
- [16] F. Eyben, K. R. Scherer, B. W. Schuller, J. Sundberg, E. André, C. Busso, L. Y. Devillers, J. Epps, P. Laukka, S. S. Narayanan, and K. P. Truong, "The Geneva minimalistic acoustic parameter set (GeMAPS) for voice research and affective computing," *IEEE Trans. Affect. Comput.*, vol. 7, no. 2, pp. 190–202, 2016.
- [17] J. Kim, S. Kim, J. Kong, and S. Yoon, "Glow-TTS: A generative flow for text-to-speech via monotonic alignment search," in *Proc. NeurIPS*, vol. 33, 2020, pp. 8067–8077.
- [18] F. Lux, J. Koch, and N. T. Vu, "Low-resource multilingual and zero-shot multispeaker TTS," in *Proc. ACL/IJCNLP*, 2022, pp. 741–751.
- [19] J. Kong, J. Kim, and J. Bae, "HiFi-GAN: Generative adversarial networks for efficient and high fidelity speech synthesis," in *Proc. NeurIPS*, vol. 33, 2020, pp. 17 022–17 033.
- [20] J. Shen, R. Pang, R. J. Weiss, M. Schuster, N. Jaitly, Z. Yang, Z. Chen, Y. Zhang, Y. Wang, R. J. Skerry-Ryan, R. A. Saurous, Y. Ajiomyriannakis, and Y. Wu, "Natural TTS synthesis by conditioning WaveNet on Mel spectrogram predictions," in *Proc. ICASSP*, 2018, pp. 4779–4783.
- [21] V. Popov, I. Vovk, V. Gogoryan, T. Sadekova, and M. Kudinov, "Grad-TTS: A diffusion probabilistic model for text-to-speech," in *Proc. ICML*, 2021, pp. 8599–8608.
- [22] Y. A. Li, A. Zare, and N. Mesgarani, "StarGANv2-VC: A diverse, unsupervised, non-parallel framework for natural-sounding voice conversion," in *Proc. Interspeech*, 2021, pp. 1349–1353.
- [23] E. Casanova, J. Weber, C. D. Shulby, A. C. Junior, E. Gölge, and M. A. Ponti, "YourTTS: Towards zero-shot multi-speaker tts and zero-shot voice conversion for everyone," in *Proc. ICML*, 2022, pp. 2709–2720.
- [24] A. Łańcucki, "FastPitch: Parallel text-to-speech with pitch prediction," in *Proc. ICASSP*, 2021, pp. 6588–6592.
- [25] E. A. AlBadawy and S. Lyu, "Voice conversion using speech-to-speech neuro-style transfer," in *Proc. Interspeech*, 2020, pp. 4726–4730.
- [26] J. Kim, J. Kong, and J. Son, "Conditional variational autoencoder with adversarial learning for end-to-end text-to-speech," in *Proc. ICML*, 2021, pp. 5530–5540.
- [27] A. Baevski, Y. Zhou, A. Mohamed, and M. Auli, "Wav2vec 2.0: A framework for self-supervised learning of speech representations," in *Proc. NeurIPS*, 2020.
- [28] X. Wang and J. Yamagishi, "Investigating self-supervised front ends for speech spoofing countermeasures," in *Proc. Odyssey: The Speaker and Language Recognition Workshop*, 2022.
- [29] J. M. Martín-Doñas and A. Álvarez, "The Vicomtech audio deepfake detection system based on wav2vec2 for the 2022 ADD challenge," in *Proc. ICASSP*, 2022, pp. 9241–9245.
- [30] H. Tak, M. Todisco, X. Wang, J. Jung, J. Yamagishi, and N. W. D. Evans, "Automatic speaker verification spoofing and deepfake detection using wav2vec 2.0 and data augmentation," in *Proc. Odyssey: The Speaker and Language Recognition Workshop*, 2022.
- [31] Y. Yang, H. Qin, H. Zhou, C. Wang, T. Guo, K. Han, and Y. Wang, "A robust audio deepfake detection system via multi-view feature," in *Proc. ICASSP*, 2024, pp. 13 131–13 135.
- [32] Y. Guo, H. Huang, X. Chen, H. Zhao, and Y. Wang, "Audio deepfake detection with self-supervised wavLM and multi-fusion attentive classifier," in *Proc. ICASSP*, 2024, pp. 12 702–12 706.
- [33] D. Kumar, P. K. V. Patil, A. Agarwal, and S. M. Prasanna, "Fake speech detection using openSMILE features," in *Proc. SPECOM*, 2022, pp. 404–415.
- [34] J. Kominick and A. W. Black, "The CMU Arctic speech databases," in *Proc. SSW*, 2004, pp. 223–224.
- [35] H. Zen, V. Dang, R. Clark, Y. Zhang, R. J. Weiss, Y. Jia, Z. Chen, and Y. Wu, "LibriTTS: A corpus derived from LibriSpeech for text-to-speech," in *Proc. Interspeech*, 2019, pp. 1526–1530.
- [36] K. Ito and L. Johnson, "The LJ speech dataset," <https://keithito.com/LJ-Speech-Dataset/>, 2017.
- [37] R. S. TN, A. Agarwal, and S. M. Prasanna, "Fake speech detection in domain variability scenario," in *Proc. National Conference on Communications*, 2024, pp. 1–6.
- [38] X. Wang, J. Yamagishi, M. Todisco, H. Delgado, A. Nautsch, N. W. D. Evans, M. Sahidullah, V. Vestman, T. Kinnunen, K. A. Lee, L. Juvela, P. Alku, Y. Peng, H. Hwang, Y. Tsao, H. Wang, S. L. Maguer, M. Becker, and Z. Ling, "ASVspoof 2019: A large-scale public database of synthesized, converted and replayed speech," *Comput. Speech Lang.*, vol. 64, p. 101114, 2020.
- [39] N. M. Müller, F. Dieckmann, and J. Williams, "Attacker attribution of audio deepfakes," in *Proc. Interspeech*, 2022, pp. 2788–2792.
- [40] J. Xue, C. Fan, Z. Lv, J. Tao, J. Yi, C. Zheng, Z. Wen, M. Yuan, and S. Shao, "Audio deepfake detection based on a combination of F0 information and real plus imaginary spectrogram features," in *Proc. Workshop on Deepfake Detection for Audio Multimedia*, 2022, pp. 19–26.
- [41] H. Tak, J. Patino, A. Nautsch, N. W. D. Evans, and M. Todisco, "An explainability study of the constant Q cepstral coefficient spoofing countermeasure for automatic speaker verification," in *Proc. Odyssey: The Speaker and Language Recognition Workshop*, 2020, pp. 333–340.
- [42] J. Yang, R. K. Das, and H. Li, "Significance of subband features for synthetic speech detection," *IEEE Trans. Inf. Forensics Secur.*, vol. 15, pp. 2160–2170, 2020.
- [43] D. Salvi, P. Bestagini, and S. Tubaro, "Towards frequency band explainability in synthetic speech detection," in *Proc. EUSIPCO*, 2023, pp. 620–624.
- [44] D. Salvi, T. S. Balcha, P. Bestagini, and S. Tubaro, "Listening between the lines: Synthetic speech detection disregarding verbal content," *arXiv preprint arXiv:2402.05567*, 2024.
- [45] N. Klein, T. Chen, H. Tak, R. Casal, and E. Khoury, "Source tracing of audio deepfake systems," in *Proc. Interspeech*, 2024.